JOURNAL OF APPLIED ELECTROCHEMISTRY 22 (1992) 613–619

Local mass transport effects in the FM01 laboratory electrolyser

C. J. BROWN, D. PLETCHER

Department of Chemistry, University of Southampton, Southampton SO9 5NH, Great Britain

F. C. WALSH

Department of Chemistry, Portsmouth Polytechnic, Portsmouth PO1 2DT, Great Britain

J. K. HAMMOND, D. ROBINSON

ICI Chemicals & Polymers Limited, Research and Development Department, P.O. Box 8, The Heath, Runcorn, Cheshire WA7 4QD, Great Britain

Received 1 August 1991; revised 14 October 1991

A number of patterns of segmented line electrodes have been manufactured using copper printed circuit board technology. These segmented electrodes have been used to investigate local mass transport effects in ICI's FM01-LC parallel plate electrolyser. It is shown that in the absence of a turbulence promoter the current distribution is uneven. Along the direction of electrolyte flow, a tertiary current distribution is observed. In addition, close to the cell entrance, an uneven current distribution occurs perpendicular to the direction of electrolyte flow; this reflects the design of the electrolyte distributor. With a turbulence promoter the current distribution is more even and the entry effects are much reduced. The turbulence promoter can, however, impose its own pattern on the current distribution perpendicular to the flow.

1. Introduction

Many electrochemical processes are operated under limiting current conditions to maximize the space time yield of the electrolyser. Mass transport therefore determines the rate of conversion of reactant to product and it is common to use inert turbulence promoters and/or high fluid velocities to enhance the mass transport to the electrode surface and, hence, the current density.

It has been common to characterize mass transport in terms of space averaged parameters estimated from measurements of the cell current under appropriate conditions [1–4]. Moreover, most laboratory studies [5–8] have employed cells with long entrance and exit zones in order to produce a fully developed flow within the interelectrode gap. In this way, results obtained for laminar flow can be correlated by the Leveque equation [9]. In contrast, most pilot scale and commercial electrolysers have short inlet and outlet zones and the fluid flow may never reach a fully developed state before leaving the cell. Turbulence promoters are commonly employed both to enhance the rate of supply of reactant to the electrode and to improve the uniformity of the mass transport conditions within the cell.

The investigation of local mass transport conditions within cells is more difficult and such studies have received little attention. They are, however, critical to an understanding of the characteristics and performance of commercially available electrolysers. A few papers have reported the use of minielectrodes [5, 6] for studies in cells with long entrance lengths, but they have several disadvantages; the construction of a large number of electrodes can be difficult and reproducibility can be poor. Moreover, they can also suffer from edge effects; as point sources they do not give a representative picture of local distributions for systems that have a two dimensional dependence on mass transport [10]. Recently, Wragg and Leontaritis [11] have reported a detailed study of mass transport in baffled and unbaffled parallel plate cells using arrays of 36, 1 mm diameter electrodes. By design of an electrode with three such arrays which could be mounted in the cell in several orientations it was possible to minotor the local mass transport at 324 points within the cell.

The construction of segmented electrodes using copper printed circuit board (PCB) technology is not new [12] but the scope of this approach for detailed studies does not seem to have been fully appreciated. Certainly, the PCB technology allows the rapid manufacture of a wide range of segment patterns by a procedure which is highly reproducible. Moreover, the electrodes are cheap and may be regarded as disposable. The method is clearly superior to other techniques [13–18] which usually involve the tedious machining of insulated electrode blocks. It should, however, be noted that the series of segmented electrodes may only approximate to the continuous plate electrode it seeks to model. With some orientations of segmented electrodes, the solution flows over repeated

0021-891X/92

areas of active and inactive surface giving rise to a complex situation where the mass transport boundary layer alternatively develops and dissipates. It is therefore necessary to select the dimensions of the segment pattern so that it is an acceptable model for the flat plate electrode. In addition, it should be recognized that the fabricated segmented structure is not completely flat since the copper strips have the thickness of the copper layer on the printed circuit board, here 40 μm.

In the earlier study [12], the copper circuit board was plated with nickel to obtain an electrode surface suitable for potassium ferricyanide reduction. In this present work, the copper itself was used as the electrode and the reduction of aqueous cupric ions in an acid medium was used as the study system. The technique is applied to the examination of local mass transport in a commerially available laboratory electrolyser, the FM01-LC unit supplied by ICI [19]; it is demonstrated that the use of several patterns of electrodes allows an unusually detailed picture of local mass transport conditions to be built up. Studies of space averaged mass transport have been reported elsewhere [20, 21].

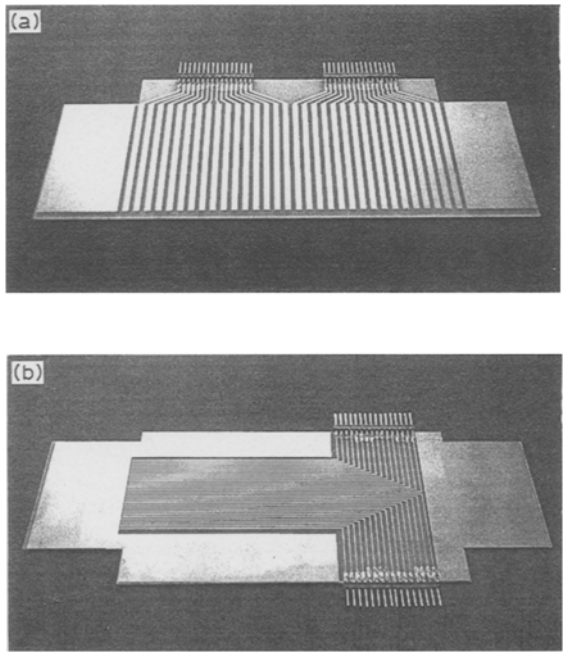

Fig. 1. (a) An example of a type V segmented electrode. Each vertical copper electrode is 0.3 cm wide with an inert spacing of 0.2 cm in between each parallel strip. (b) An example of a type H segmented electrode. Each horizontal copper electrode is 0.6 mm wide with inert spacings of 0.6 mm between each.

2. Experimental details

2.1. *Flow circuit and electrochemical cell*

The flow circuit consisted of a 1000 cm^3 reservoir, a thermostat (Tecan), a glass rotameter with a stainless steel float (KDG X14 M) and a pump (Totton EMP 40/4). All interconnecting tubing was of silicone rubber (mostly 7 mm internal diameter).

The parallel plate electrolyser used for this series of experiments was an ICI FM01-LC unit [19]. The electrolyte flows across an electrode 16 cm long and 4 cm high (B) and the electrolyte channel, formed by a combination of spacers and gaskets, gave an inter-electrode gap (S) of 5.5 mm after the end plates were uniformly compressed to a torque of 25 N m. These dimensions lead to a hydraulic diameter ($d_e = 2BS/(B + S)$) of 0.97 cm. Electrolyte flow to the channel was achieved by internal manifolding which distributed the flow. The flow rate was controlled in the range 0.3 to 1.5 $dm^3 min^{-1}$, corresponding to a calculated mean linear velocity of between 2.4 to 11.2 $cm s^{-1}$ in the empty channel. The temperature was controlled at 298 $\pm$ 0.5 K.

2.2. *Electrodes and promoters*

The segmented copper electrodes were produced using a standard printed circuit board technique. An ultraviolet sensitive copper clad board was masked before it was exposed to u.v. radiation from a mercury lamp. The exposed, unwanted areas of copper were etched away by immersing the board in a ferric chloride solution. A mask of the required pattern was produced with the help of a Ranger software package supplied by Seetrax Ltd. Two types of electrodes were produced: (i) type V consisted of vertical, parallel electrodes used to study the current distribution along the direction of the electrolyte flow. For example, Fig. 1a shows an electrode with 32 parallel copper strips, 3 mm wide with inert spacings of 2 mm between; and (ii) type H consisted of 32 horizontal, parallel copper strips, 0.6 mm wide with inert spacings of 0.6 mm between. This electrode was used to study the current distribution across the electrolyte flow (Fig. 1b). Several electrodes of type H were produced with various active electrode lengths, by masking the unwanted area with an isolating film; this enabled the study of discrete sections of the cell channel.

The manufacturer's data sheet stated the copper thickness to be 40 μm. The prepared electrode boards were supported on a 15 mm thick perspex plate, which also held the external connection blocks for the electrodes. The anode used with both types of electrode was a flat copper plate in order to maintain the concentration of Cu^{2+} in the solution at a constant level.

Two types of turbulence promoters were used in this study. Type A was a mesh (Fig. 2a), made from high density polyethylene. It had an overall thickness of 5.5 mm with both a short and long diagonal of 9.5 mm. Inserted into the electrolyte channel, it gave an approximate open area of 60% [19]. Type B was a stack of 8 fine plastic nets with 1 mm squares. Figure 2b shows a single net. The number in the stack was selected so that, when compressed in the cell, the overall thickness was again 5.5 mm.

2.3. *Instrumentation and current measurement*

Potentiodynamic and potentiostatic techniques were used for this study. To achieve potential control of the

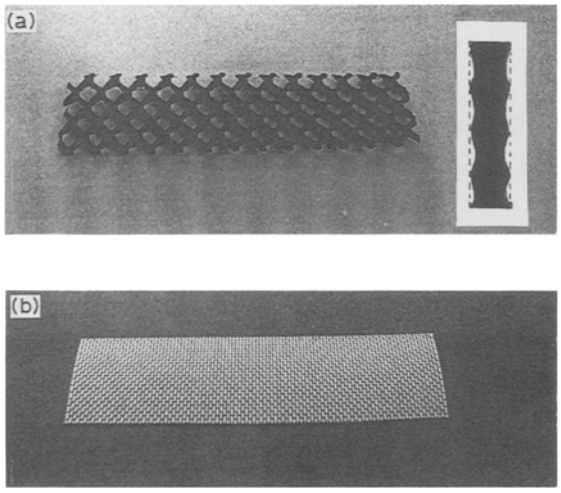

Fig. 2. (a) A type A turbulence promoter of blown polyethylene. The inset shows the edge profile. (b) The 1 mm polymer net used for the preparation of the type B turbulence promoter.

working segmented electrodes, a capillary tube was inserted into the wall of the spacer, which made electrical contact with the SCE reference electrode (Radiometer type K401). A schematic of the electronic circuit is shown in Fig. 3. The potential was controlled by a HiTek DT2101 potentiostat and PPR1 waveform generator. When required, current-potential curves were recorded on a Gould 60000 series chart recorder. A multichannel V/MOSFET current follower was constructed to give an output voltage proportional to the current flowing through each electrode. The electrodes were multiplexed into groups of eight for each operational amplifier, which incorporated an individual gain setting of 10^{-5} to 10^{-2} A V^{-1}. The V/MOSFET switching system allowed one electrode from each group of eight to be read via its operational amplifier, whilst the other electrodes in the cell remained active, i.e. still passing current. The outputs from the operational amplifiers were connected to a multichannel interface. This interface comprized a fast 12-bit analogue to digital converter and a digital output to control the current follower. The interface was connected via a 1 MHz bus to a Master BBC Micro-

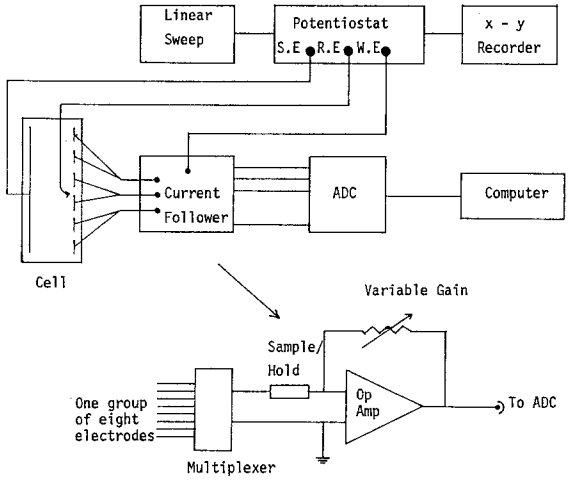

Fig. 3. Schematic diagram of the electronic circuit used for determining current distributions within the cell.

Table 1. Physical properties of the solution: 0.005 M copper (II) in aqueous 1.5 M H_2SO_4 at 298 K.

Density, ρ	1.096 g cm^{-3}
Dynamic viscosity, η	0.0119 g cm^{-1} s^{-1}
Schmidt number, $\eta/\rho D$	2172
Diffusion coefficient for Cu(II), D	5.0×10^{-6} cm^2 s^{-1}

computer which was used to control the experiment and collect the data. To minimize random errors due to voltage fluctuations, each electrode was read twenty times with an averaged value being calculated by the computer. A constant cathode voltage of −0.35 V/SCE) was maintained during all current measurements using the segmented electrodes.

2.4. *Experimental procedure*

A fresh solution of 0.005 M copper sulphate (BDH, Analar) in 1.5 M sulphuric acid (Interchem, AR) was used for each experiment. Before the cell was assembled, the electrodes were prepared using wet 1200 grade emery paper and polished with alumina powder before being washed with distilled water and degreased with acetone. After assembly the flow system was loaded with the working electrolyte and purged with nitrogen for 20 min, with continuous purge being maintained on the closed reservoir during the course of the experiment. Physical properties for the electrolyte are reported in Table 1. Using these quantities, it may be shown that the flow rates employed correspond to Reynolds numbers between 212 and 855.

The mass transport coefficient, k_L was calculated from the limiting current density, j_L, using the equation

$$k_L = j_L/2Fc$$

The limiting current density was calculated by dividing the limiting current by the projected electrode area, A.

3. Results and discussion

3.1. *Preliminary experiments*

Current–potential curves were recorded at a series of flow rates for a solution of 5 mM Cu(II) in 1.5 M sulphuric acid at (a) at flat plate copper electrode of area 64 cm^2 and (b) a type V segmented electrode, total area 38.4 cm^2 (all segments active). The experiments were carried out both with and without turbulence promoters in the cell. Figure 4 shows typical curves, in fact, recorded at the segmented electrode without a turbulence promoter in the cell. All the curves show waves for the reduction of cupric ion to copper metal with a well defined limiting current plateau extending over a potential range of at least 500 mV. The limiting currents were measured at −0.35 V/SCE and used to construct the plots of mass transfer coefficients versus linear flow rate shown in Fig. 5. It can be seen that there is no significant difference between the mass

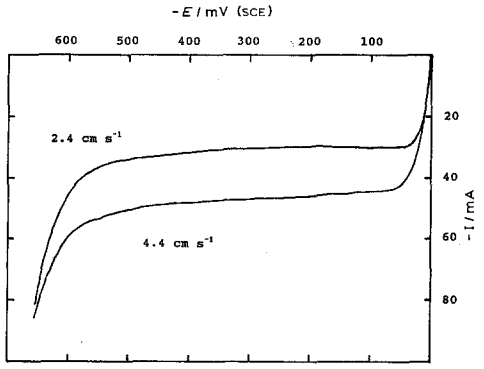

Fig. 4. Total I–E responses for the type V copper segmented electrode in 0.005 M copper (II) + nitrogen purged 1.5 M H_2SO_4. Potential scan rate 3 mV s^{-1} with T = 298 K.

transfer coefficients at the flat plate and the segmented electrode, whether or not there is a type A turbulence promoter in the cell. The turbulence promoter, however, markedly enhances the rate of mass transport to both the flat plate and segmented electrodes. Figure 5 also shows one set of data for the type B turbulence promoter and it can be seen that the stack of nets is a more efficient promoter than type A. The slopes of the log k_L against log v plots are all close to 0.58. The similarity in the log k_L against log v plots for the segmented and flat plate electrodes implies that the mass transport regimes at the former is a reasonable model for the continuous active surface. In addition, it appears that the 40 μm steps on the surface of the segmented electrode, resulting from the method of manufacture, do not distort the mass transport regime to any significant extent.

3.2. *Measurements of local mass transport*

In the first set of experiments, a type V electrode with 32 vertical 3 mm wide segments separated by 2 mm gaps was used. Limiting currents were recorded individually for each of the 32 segments (again using the 5 mM solution of Cu(II) in 1.5 M H_2SO_4 and a potential

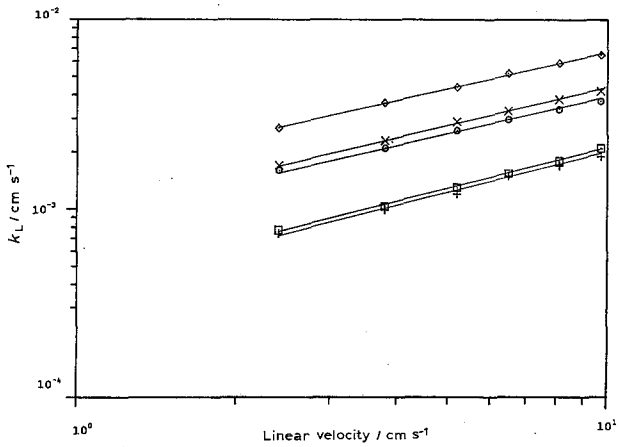

Fig. 5. Double logarithmic plot of the mass transport coefficient, k_L, against linear electrolyte flow velocity for: a copper flat plate electrode with type A promoter (○); a segmented copper electrode with turbulence promoters – type A (×) and type B (◇); and electrodes without promoters – segmented (□) and homogeneous flat plate (+). Solution: 0.005 M copper (II) in nitrogen purged 1.5 M H_2SO_4. Limiting currents measured at −0.35 V/SCE with T = 298 K.

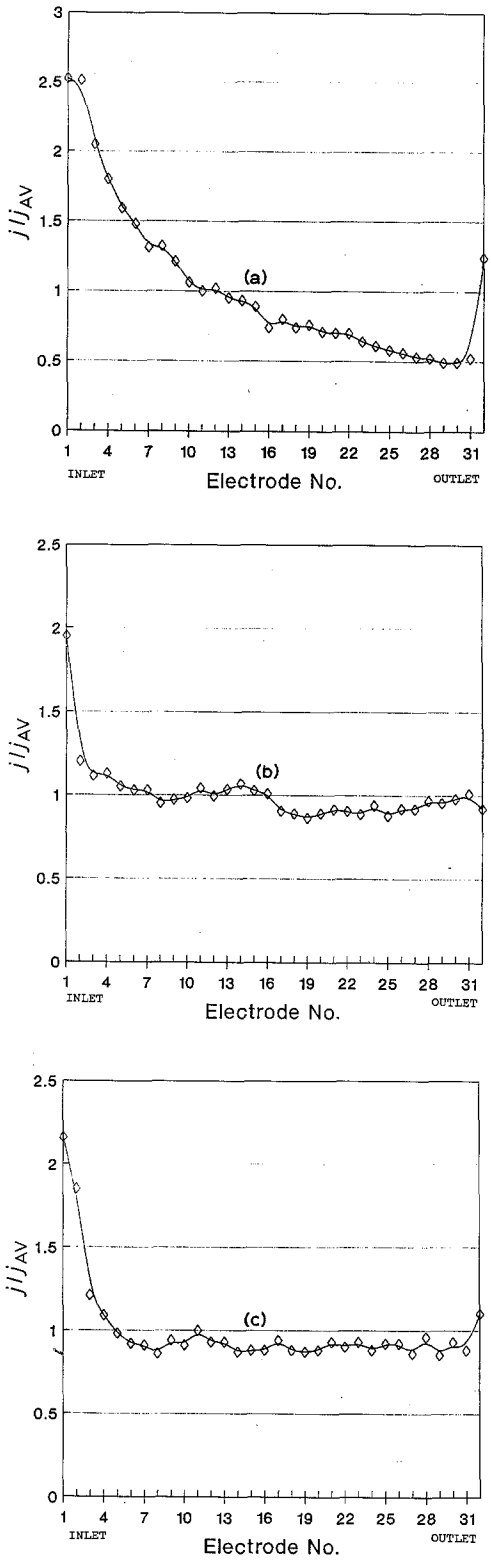

Fig. 6. Current distributions along the direction of solution flow determined with type V copper segmented electrodes: (a) no turbulence promoter (b) type A turbulence promoter (c) type B turbulence promoter. Single segment size = 0.3 cm × 4 cm. Solution 0.005 M copper(II) in nitrogen purged 1.5 M H_2SO_4. Limiting currents measured at −0.35 V/SCE with T = 298 K. Electrolyte flow rate of 6.5 cm s^{-1}.

of −0.35 V/SCE) at six electrolyte flow rates between 2.4 and 9.7 cm s^{-1}. The experiments were carried out both with an empty channel and with turbulence promoters.

Figure 6a shows a current distribution for the parallel plate cell when the channel is empty and the

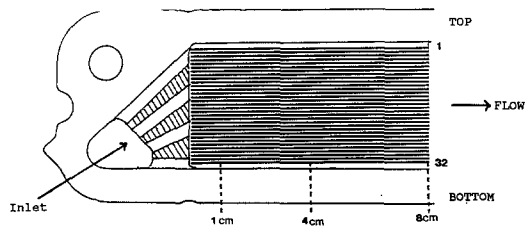

Fig. 7. Schematic diagram representing the pattern for the horizontal, segmented electrode (type H) in relation to the inlet manifold channels.

electrolyte flow rate is $6.5\,cm\,s^{-1}$. The data are presented as a plot of j/j_{AV} against segment number from the electrolyte inlet; j_{AV} is the average current density over the 32 segments. It can be seen that the current density is very high at the inlet and drops continuously across the electrode except for the final electrode. The form of the plot is that expected for a tertiary current distribution [1–4]. The electroactive species is depleted within the mass transport layer and its concentration at the surface of the electrode surface drops along the length of the electrode. The increase in the value for the last electrode may be attributed to its proximity to the cell outlet where the electrolyte flow meets the edge of the spacer leading to some turbulence.

The results when a type A turbulence promoter is included in the flow channel, see Fig. 6b, show a very marked improvement in the current distribution. The entrance effect is limited to the first three segments (< 10% of the cell length) and the current distribution is almost uniform over the rest of the cell. With the type B turbulence promoter, with the finer mesh, the entry zone is further diminished, see Fig. 6c. Clearly, the turbulence promoters are very successful in creating the turbulence to mix the bulk and transport layer phases and there is no marked drop in the Cu(II) concentration along the electrode. The current distributions, in the dimensionless form of Fig. 6, show no dependence on the electrolyte flow rate.

Visual inspection of the segmented electrode after the above experiments showed there to be a variation in the distribution of deposited copper down the vertical segments near the inlet of the cell. Hence, a second series of experiments was carried out using type H electrodes where the segments are horizontal strips along the direction of flow. As above, experiments were performed both with and without a turbulence promoter and as a function of electrolyte flow rate. Three electrodes of type H were constructed with different active electrode lengths of 8, 4 and 1 cm (Fig. 7). In each case, the surface of the copper/printed circuit board downstream of the active electrode area was masked with a thin layer of epoxy resin.

Figure 8 shows the current distribution across the electrolyte flow, measured with the 1 cm electrodes, when the cell is operated without a turbulence promoter for three flow rates (electrode 1 is situated at the top of the cell). It can be seen that the current distribution is uneven close to the cell entrance. There are effectively four "jet streams" with three relatively stag-

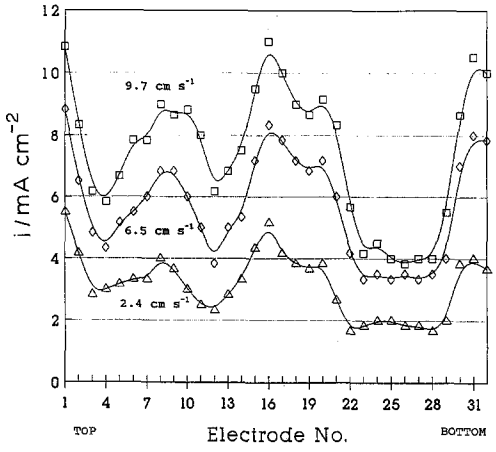

Fig. 8. Influence of the electrolyte flow rate on the current distribution across the flow at the entry to the cell, measured with 1 cm, type H segmented electrodes. No turbulence promoter. Single segment size = 1.0 cm × 0.6 mm. Solution 0.005 M copper(II) in nitrogen purged 1.5 M H_2SO_4. Limiting currents measured at −0.35 V/SCE with T = 298 K.

nant zones between. The general form of this current distribution is readily understood in terms of the way the electrolyte enters the channel. The internal manifold, see Fig. 7, is designed with four electrolyte inlets, angled across the cell entrance. This would be expected to cause the flow to be divided into four streams and, hence, alternating areas of high and low flow (turbulence) are observed. Jetting along the walls of the cell from the manifold gives rise to higher current densities in these regions as shown by electrode numbers 1–3 and 28–32.

The development of the flow pattern as the electrolyte passes through the cell is shown in Fig. 9. This figure reports the variation in current density across the flow as measured with the three electrodes with lengths of 8, 4 and 1 cm, at the same flow rate of $6.5\,cm\,s^{-1}$. This clearly shows that on moving away from the inlet, the distribution caused by the manifold gradually diminishes, although some variation is still seen for the 8 cm electrode which reaches to the half way point of the cell. By this stage, the flow pattern is

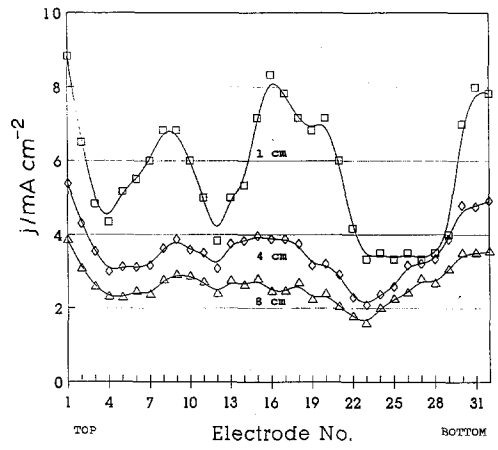

Fig. 9. Current distributions across the flow, measured with different length, type H segmented electrodes. No turbulence promoter. Solution: 0.005 M copper(II) in nitrogen purged 1.5 M H_2SO_4. Limiting currents measured at −0.35 V/SCE with T = 298 K. Electrolyte flow rate of $6.5\,cm\,s^{-1}$.

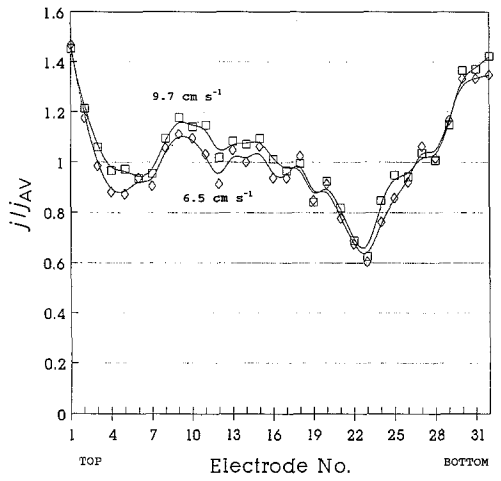

Fig. 10. Current distributions across the flow as a function of electrolyte flow rate, measured with 8 cm, type H segmented electrodes. No turbulence promoter. Solution: 0.005 M copper(II) in nitrogen purged 1.5 M H_2SO_4. Limiting currents measured at -0.35 V/SCE with $T = 298$ K.

very difficult to predict since it will arise from complex interactions between the initial four entry streams. The form of the current distribution again has little dependence on flow rate as shown by a plot of j/j_{AV} against electrode position for different flow rates, see Fig. 10.

The presence of the turbulence promoter in the cell has a strong influence on the current distribution pattern. Figure 11 shows the current distribution determination with the 8 cm electrodes and a type A promoter in the electrolyte compartment. It can be seen that the current distribution shows a significant periodic variation across the direction of flow. This results from the structure of the turbulence promoter, see Fig. 2a. When it is held in the interelectrode space, the promoter has four discrete channels and there is also bypassing along the walls of the cell. The troughs of the waves are consistent with points on the electrode surface which are in contact with the promoter, and therefore not contributing as much to the activity of the electrode. Results from the 4 and 1 cm elec-

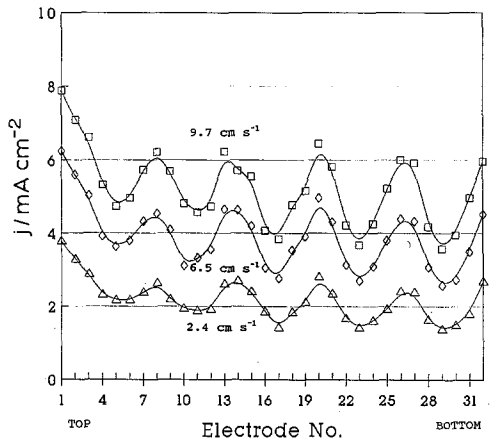

Fig. 11. Current distribution across the flow in the presence of a type A turbulence promoter as a function of electrolyte flow rate. Measurements at 8 cm, type H segmented electrodes. Solution: 0.005 M copper(II) in nitrogen purged 1.5 M H_2SO_4. Limiting currents measured at -0.35 V/SCE with $T = 298$ K.

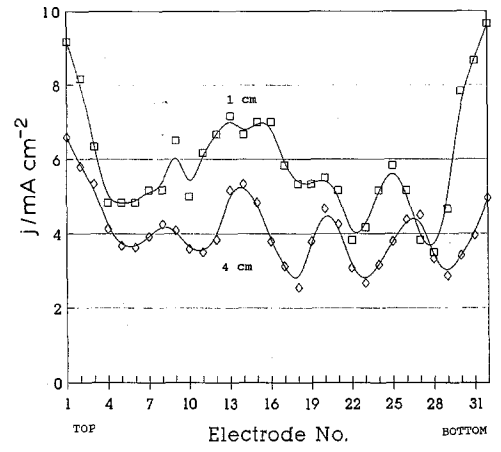

Fig. 12. Current distribution across the flow in the presence of a type A turbulence promoter measured with different length, type H segmented electrodes. Solution: 0.005 M copper(II) in nitrogen purged 1.5 M H_2SO_4. Limiting currents measured at -0.35 V/SCE with $T = 298$ K.

trodes, see Fig. 12, show that the above flow pattern is not immediately established, and that over the first few centimetres of the channel, the inlet manifold still contributes to the current distribution. Indeed, with the shortest electrodes, the current distribution still mirrors that without the turbulence promoter, *cf.* Fig. 8.

The type B turbulence promoter with the finer mesh does not impose its own flow pattern to the same extent. Figure 13a and b compare the current distribution measured with the 8 cm electrodes with type A and type B turbulence promoter. Moreover, it can be seen from the distributions measured with the shorter electrodes, Figs 8 and 12, that the turbulence promoter significantly smooths the flow streams resulting from the electrolyte distributor.

4. Conclusions

The manufacture of segmented electrodes using printed circuit board technology provides a convenient and versatile method to make segmented electrodes. The complexity of the electrode pattern is largely limited by the imagination of the experimental worker, not the difficulty in manufacturing the segmented electrode, and this allows a much more detailed examination of local variations in mass transport.

In this study, the technique has been used to subject the FM01-LC electrolyser to critical examination and it is shown to perform well. It is, however, essential to use a turbulence promoter to avoid large variations in current distribution both (a) along the direction of flow due to depletion of the electroactive species within the boundary layer at the electrode surface and (b) across the direction of flow due to the design of the electrolyte distributor. This would, however, surely be the case with all parallel plate electrolysers without long entry and exit lengths, i.e. all commercial electrolysers. Turbulence promoters lead to a worthwhile increase in the overall mass transport coefficient and also cause the major unevenness in current distri-

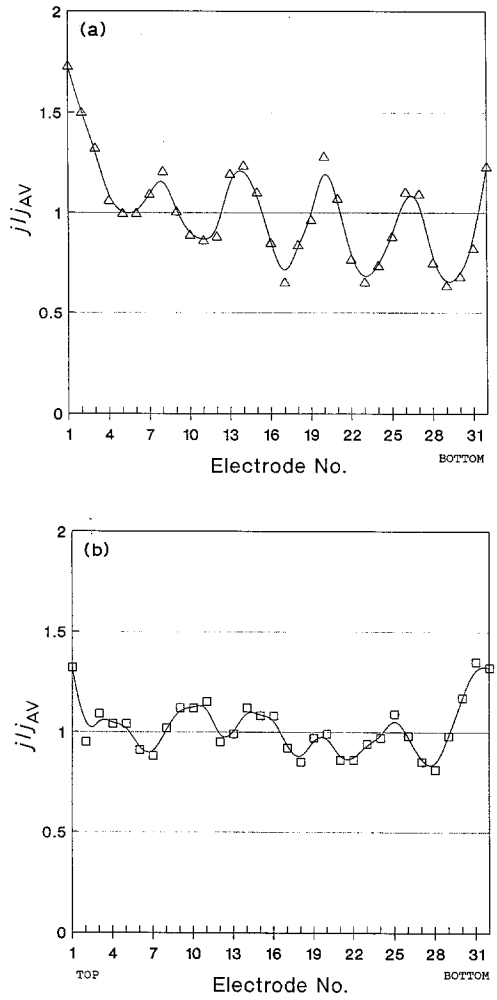

Fig. 13. Comparison of the current distributions resulting from the presence of (a) type A and (b) type B turbulence promoters. Measurements with 8 cm, type H segmented electrodes. Solution: 0.005 M copper(II) in nitrogen purged 1.5 M H_2SO_4. Limiting currents measured at -0.35 V/SCE with $T = 298$ K. Electrolyte flow rate 2.4 cm s^{-1}.

bution to be limited to a short zone close to the entrance, perhaps 10% of the electrode length in the present case. The turbulence promoter itself can impose a current distribution variation of up to 30%.

In all respects, the type B turbulence promoter, made from a stack of fine nets, is superior to the type A. The space averaged mass transfer coefficient is higher and the local variations measured with both the vertical and horizontal segmented electrodes are significantly smaller. This is to be expected because the type A promoter has a rather coarse structure for a small electrolyser.

Acknowledgements

The academic authors would like to thank ICI Chemicals & Polymers Ltd for financial support of this work. We also acknowledge the assistance of the Electronics Workshop in the Chemistry Department, University of Southampton in the design of the current follower system and the software for its interference to the computer.

References

[1] J. S. Newman, 'Electrochemical Systems', Prentice-Hall, Englewood Cliffs, NJ (1973).
[2] D. J. Prickett, 'Electrochemical Reactor Design', Elsevier, Amsterdam (1979).
[3] F. Coeuret and S. Storck, 'Eléments de Genie Electrochimique', Tecdoc, Paris (1984).
[4] D. Pletcher and F. C. Walsh, 'Industrial Electrochemistry', Chapman & Hall, London (1990).
[5] F. Schwager, P. M. Robertson and N. Ibl, *Electrochim. Acta* **25** (1980) 1655.
[6] A. Storck and D. Hutin, *ibid.* **26** (1981) 127.
[7] F. B. Leitz and L. Marincic, *J. Appl. Electrochem.* **7** (1977) 473.
[8] R. E. W. Jansson and R. J. Marshall, *Electrochim. Acta* **27** (1982) 823.
[9] J. R. Selman and C. W. Tobias, *Adv. Chem. Eng.* **10** (1978) 1.
[10] F. Goodridge, G. M. Mamoor and R. E. Plimley, IChemE Symposium Series No. 98 (1985) p. 61.
[11] A. A. Wragg and A. A. Leontaritis, 'Electrochemical Cell Design and Optimisation', Dechema Monograph, **123** (1991) 345.
[12] A. Storck and F. Coeuret, *Electrochim. Acta* **22** (1977) 1155.
[13] C. W. Tobias, M. Eisenberg and C. R. Wilke, *J. Electrochem. Soc.* **99** (1952) 359R.
[14] U. Landau, *AIChE Symposium Series, No. 244*, **77** (1981) 75.
[15] W. W. Focke, *Electrochim. Acta* **28** (1983) 1137.
[16] A. Palade De Iribarne, S. L. Marchiano and A. J. Arvia, *ibid.* **15** (1970) 1827.
[17] Qi Jian and R. F. Savinell, *J. Appl. Electrochem.* **20** (1990) 885.
[18] L. R. Czarnetzki and J. J. Janssen, *ibid.* **19** (1989) 630.
[19] D. Robinson, in 'Electrosynthesis – from laboratory, to pilot, to production' (edited by J. D. Genders and D. Pletcher), The Electrosynthesis Co., Buffalo, NY (1990).
[20] C. J. Brown, D. Pletcher, F. C. Walsh, J. K. Hammond and D. Robinson, Dechema Monograph, **123** (1991) 299.
[21] *Idem* submitted to *Journal of Applied Electrochemistry*.